

NiTi microstructure evolution by *in situ* Neutron Diffraction

Zifan Wang, Jingwei Chen, Cyril Besnard, Alexander M. Korsunsky*

MBLEM, Department of Engineering Science, University of Oxford, Oxford OX1 3PJ, U.K.

*Corresponding author. E-mail address: alexander.korsunsky@eng.ox.ac.uk

DOI: <https://doi.org/10.1016/j.matlet.2020.128676>

Received 10 August 2020, Accepted 11 September 2020, Available online 13 September 2020.

Abstract

Cold-worked NiTi wire was subjected to ageing treatment, during which *in situ* neutron diffraction technique was employed to investigate the microstructure evolution in terms of crystallinity, precipitation, texture, grain size and microstrain. It was found that both heating and rapid cooling brings about significant change in microstructure, whilst precipitation process is dominant at high temperature. Besides, the approaches to extracting microstructural information, including texture, grain size and microstrain, from individual neutron diffraction pattern are proposed and verified.

Keywords:

NiTi shape memory alloys, *In situ* neutron diffraction, Heat treatment, Microstructure

1. Introduction

Among the category of shape memory alloys, near-equiatomic NiTi always remains the first choice in engineering application due to its excellent thermomechanical performance [1]. Our recent study demonstrated that ageing treatment exerts huge impact on the microstructure, thereby leading to the variation of functional properties [2]. Nevertheless, the details of microstructural evolution are not well understood, since up-to-date studies only focused on the heating process of heat treatment while cooling is neglected [3,4].

In situ neutron diffraction technique provides highly reliable statistical data from enormous gauge volume instead of local regions, thus enabling probing the microstructure at its most representative form. In the present study, probably the first attempt so far, we completely tracked the microstructure before, during and after ageing treatment, thus giving insight into the optimization of ageing treatment

conditions.

2. Experimental and analytical methods

A commercially available cold drawn binary NiTi wire (Goodfellow, Ni55/Ti45 wt%) of 0.8mm diameter was used. The as-received wire was segmented and mounted on the radiant air furnace at ENGIN-X beamline, ISIS RAL, UK. Illustrated in Fig. 1, the wire was horizontally arranged in such a way that the cylindrical axis was 45° relative to the incident beam. Two detector banks were opposed in a line perpendicular to the beam direction [5]. This setup enables probing the microstructure of grains whose hkl lattice planes are either parallel (Bank 2) or perpendicular (Bank 1) to the wire axial direction. Note that the word “(hkl) variant” has been adopted in the present study, and many others, to represent the grain family that contributes to a single hkl peak in the diffraction spectra.

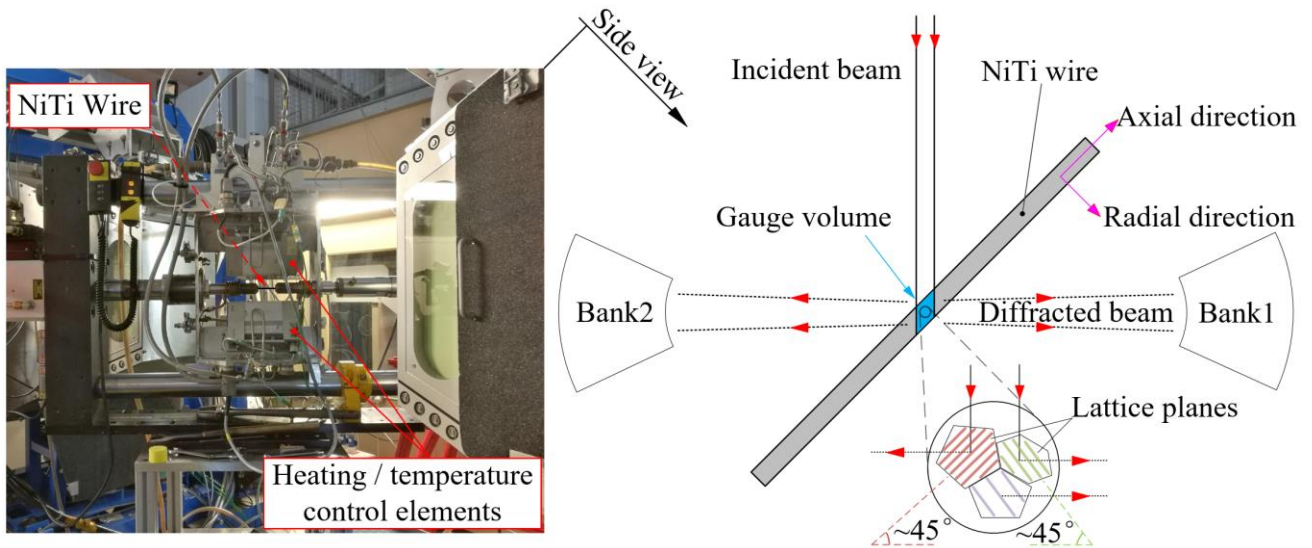


Fig. 1. Side view photo (left) and top view sketch (right) of setup.

The ageing treatment scheme is described in Fig. 2(a). The temperature quickly elevated and stabilized at 500°C . One sample was water quenched after ~ 1 hour and the other after ~ 5 hours. The time and temperature at which the diffraction spectra were collected were identified by numbers in yellow-coloured marks.

Data were analysed using Rietveld refinement technique implemented in the GSAS [6]. Raw pole figures were constructed from the refined spherical harmonics, after which the orientation distribution functions (ODFs) were reconstructed using MTEX code [7]. Hence the plotted inverse pole figures

present texture information in the axial and radial direction of the wire. Pseudo-voigt function was utilized in the single peak fitting, extracting full width half maximum (FWHM) from individual peak profile.

3. Results and discussion

3.1 Recrystallization and precipitation

Cold drawing introduces a large amount of amorphous phase with embedded nano-crystalline regions in the NiTi alloy [3]. The phenomenon is reflected in Fig. 2(b1), as both spectra show profile containing much noise caused by diffuse scattering corresponding to the amorphous phase. Only a few low-intensity peaks can be observed, implying a low degree of crystallinity. Moreover, the peaks are shifted far away from standard d-spacing positions due to the distortion of crystal structure, making it impossible to analyse via Rietveld method.

Upon heating up to 500 °C, the emergence of diffraction peaks reveals the recrystallization of amorphous phase. The peak of (111) variant is particularly intense in the wire axial direction (bank 1) whilst it is the (110) variant in the radial direction, which suggests strong texture at high temperature. There is no significant change in the microstructure during ageing treatment, judging from the comparison between Fig. 2(b2) and (b4).

After water quenching, the rising intensities of other peaks infers a more homogenous distribution of crystallite orientation, i.e. the comparison between Fig. 2(b2) and (b3). In addition to the parent phase, diffraction peaks from Ni_4Ti_3 precipitate can be observed after 5 hours' ageing treatment and water quenching, shown in Fig. 2(b5).

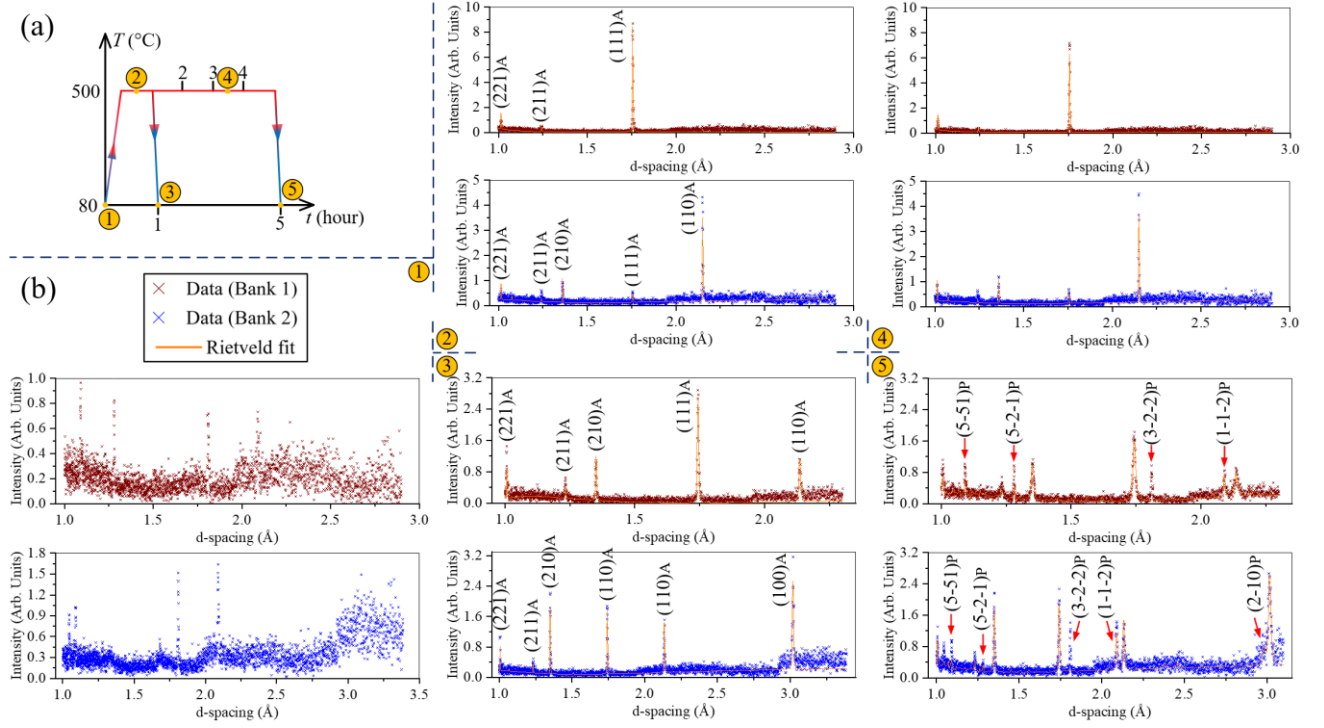


Fig. 2. Ageing treatment scheme (a) and sets of diffraction spectra of corresponding data acquisition points(b). Peaks of hkl variants are indexed for both parent austenite phase (“A”) and Ni_4Ti_3 precipitate (“P”).

3.2 Texture variation

Texture information extracted from the spectra in Fig. 2(b2-b5) is shown as inverse pole figures in Fig. 3. Units of m.r.d. is adopted, e.g. 1 m.r.d. represents random distribution and 3 m.r.d. means the quantity of a hkl variant is 3 times that of its randomly distributed state.

During the ageing treatment, the cold drawn NiTi wire exhibited strong fibre texture near $\langle 111 \rangle$ in axial direction, which is commonly reported in other studies, e.g. [8]. This agrees well with the intense (111) peak in Fig. 2(b2). In radial direction, orientation of crystallite was distributed along the direction path from $\langle 112 \rangle$ to $\langle 101 \rangle$, as indicated by the purple dash line. This implies that the crystallites were oriented in such a way homogenously rotating around the $\langle 111 \rangle$ axial texture. There is no significant variation in texture during the 5-hour period at high temperature (Fig. 3(2 and 4)).

Nevertheless, water quenching brings about huge changes in texture (Fig. 3(3 and 5)). The original texture orientation, namely $\langle 111 \rangle$ in axial direction and $\langle 101 \rangle$ in radial direction, was broadened, forming a new emphasis within the $\langle 111 \rangle \sim \langle 101 \rangle$ domain. Similarly, there is no significant variation in texture after water quenching as the ageing time increases.

Moreover, the texture of Ni_4Ti_3 precipitate is refined, shown in the 120° circular arc area according to the hexagonal symmetry of the rhombohedral structure of Ni_4Ti_3 precipitate. There is a high concentration of $\langle 0001 \rangle$ in axial direction, around which crystallite rotates homogenously so that there is an intense edge in the plot of radial direction. It can be inferred that the orientation relationship between the parent phase and precipitate is $(0001)_\text{P} \parallel (111)_\text{A}$, consistent with [9].

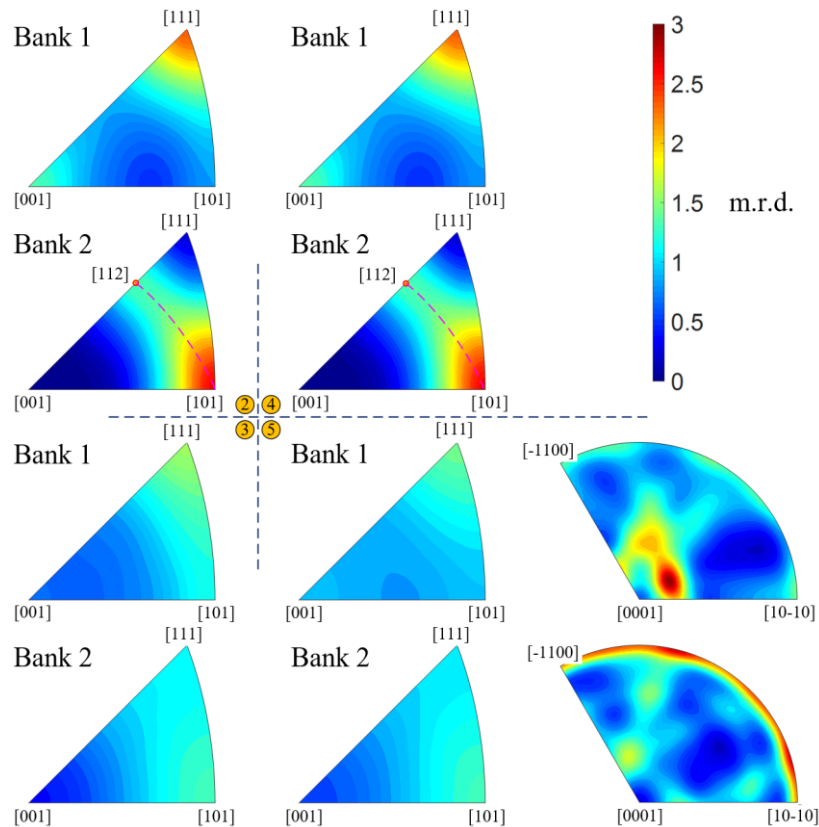


Fig. 3. Texture evolution of NiTi wire in axial (bank 1) and radial direction (bank 2). The scale of plots is normalized, ranging from 0 to 3 m.r.d.

3.3 Microstrain and grain size

To evaluate the change in microstrain, the full width at half maximum (FWHM) can be deconvoluted into multiple contributions from instrumental broadening (Δd_{ins}), grain size (Δd_{size}) and microstrain (Δd_{ϵ}) [10]. By considering the strain expression as $\epsilon = \Delta d/d$ that directly reveals the non-uniform lattice deformation from $d + \delta d$ to $d - \delta d$ for a specific hkl variant, we obtain:

$$FWHM^2 = \Delta d^2 = \Delta d_{ins}^2 + \Delta d_{size}^2 + \Delta d_{\varepsilon}^2 = \Delta d_{ins}^2 + \Delta d_{size}^2 + \varepsilon^2 d^2, \quad (1)$$

where d is the d-spacing of peak centre of a hkl variant. Eq. (1) is a typical $y=ax$ equation from which slope (ε^2) the value of microstrain can be determined by plotting Δd^2 versus d^2 , as shown in Fig.

4(a).

To evaluate the grain size, a modified Williamson-Hall approach can be used [11], written as:

$$\frac{\Delta d^2}{d^4} = \left(\frac{C}{D}\right)^2 + \frac{A}{d^2}, \quad (2)$$

where A is a constant depending on the physical properties of lattice defects that dominate the microstrain, C is the Scherrer constant which is calibrated by our EBSD study [2] and taken as 0.75, and D is the average grain (crystallite) size in unit of nm. Similarly, the ordinate intercept of a linear fitting of Eq. (2) provides the value of $(0.75/D)^2$, from which the grain size D can be calculated, as shown in Fig. 4(b).

Calculated values of microstrain and grain size are averaged between bank 1 & 2, as summarized in Fig. 4(c). The increase of grain size during ageing treatment at 500 °C is negligible, whilst the microstrain increment is attributed to the strain field arising with the nucleation and growth of precipitate [9]. The significant elevation of microstrain after water quenching results from the fragmentation of the large grains that causes intergranular constraint among smaller grains.

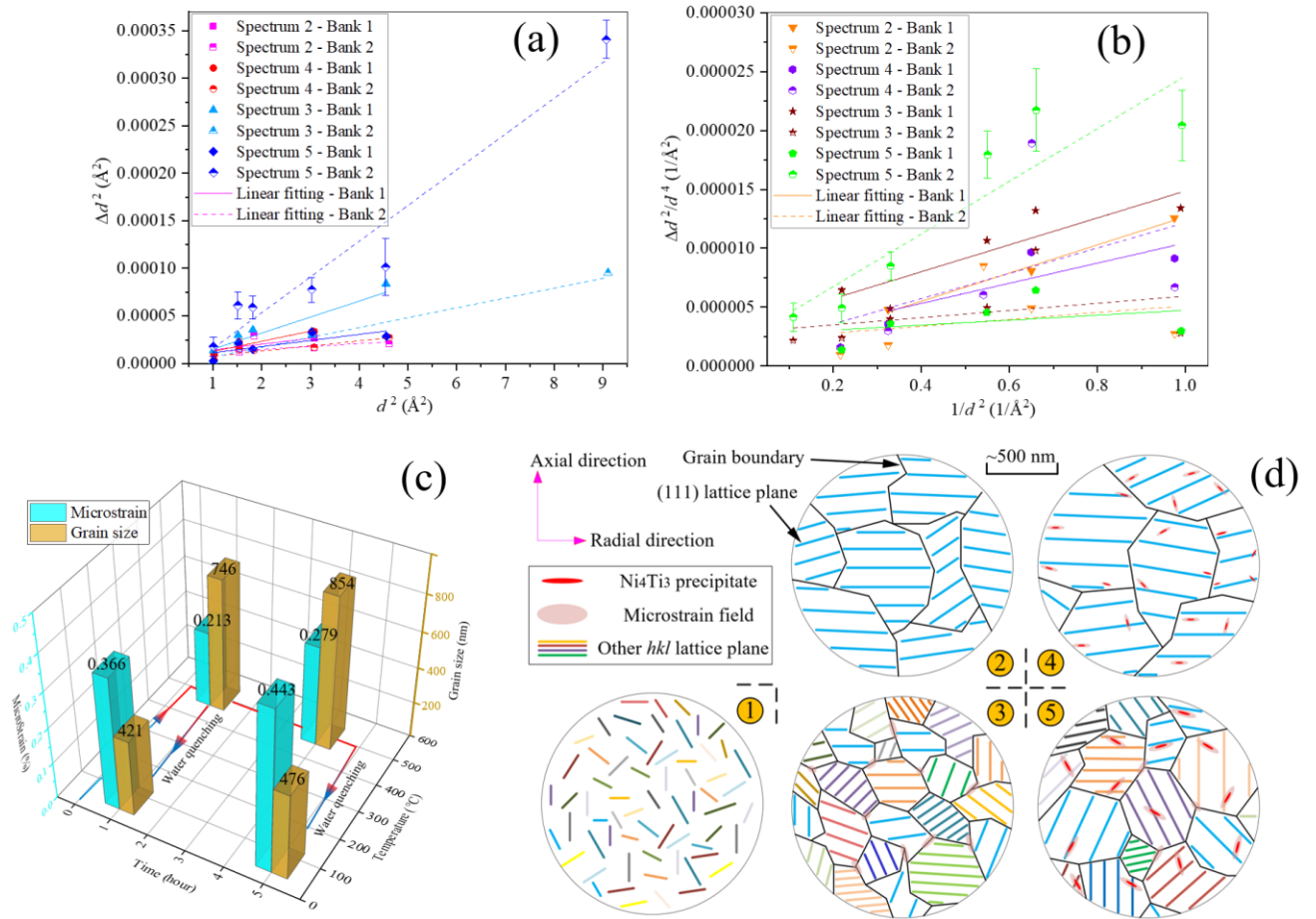


Fig. 4. Evaluation of microstrain (a) and grain size (b), results summarized in (c). Schematic illustration of microstructure evolution (d).

4. Conclusions

The volume averaged microstructure evolution of NiTi during the entire ageing treatment process was investigated. Conclusions are sketched in Fig. 4(d) and outlined as below:

- (1) The initial microstructure of as-drawn wire contains a large amount of amorphous phase. Recrystallization takes place upon heating, leading to the strong $\langle 111 \rangle$ texture in axial direction.
- (2) Precipitation is the dominant microstructural change during ageing treatment, while the change in texture and grain size is negligible.
- (3) Water quenching results in the fragmentation of large grains, hence the increase of microstrain and variation of texture.

Acknowledgements

We gratefully acknowledge the STFC for access to neutron beamtime RB1920246 at the ISIS Pulsed Neutron and Muon Source.

References

- [1] Z. Wang, A.M. Korsunsky, Effect of Temperature on Shape Memory Materials, in: Reference Module in Materials Science and Materials Engineering, Elsevier Inc., 2020.
- [2] Z. Wang, J. Everaerts, E. Salvati, A.M. Korsunsky, Evolution of thermal and mechanical properties of Nitinol wire as a function of ageing treatment conditions, *J. Alloys Compd.* 819 (2020) 153024.
- [3] C. Yu, B. Aoun, L. Cui, Y. Liu, H. Yang, X. Jiang, S. Cai, D. Jiang, Z. Liu, D.E. Brown, Y. Ren, Synchrotron high energy X-ray diffraction study of microstructure evolution of severely cold drawn NiTi wire during annealing, *Acta Mater.* 115 (2016) 35-44.
- [4] M. Carl, J. Smith, R.W. Wheeler, Y. Ren, B.V. Doren, M.L. Young, High-energy synchrotron radiation X-ray diffraction measurements during in situ aging of a NiTi-15 at. % Hf high temperature shape memory alloy, *Materialia* 5 (2019) 100220.
- [5] J.R. Santisteban, M.R. Daymond, J.A. James, L. Edwards, ENGIN-X: a third-generation neutron strain scanner, *J. Appl. Cryst.* 39 (2006) 812-825.
- [6] A.C. Larson, R.B. Von Dreele, General structure analysis system, Los Alamos National Laboratory Report LAUR (1994) 86-748.
- [7] F. Bachmann, R. Hielscher, H. Schaeben, Texture analysis with MTEX-Free and open source software toolbox, *Solid State Phenom.* 160 (2010) 63-68.
- [8] K. Gall, J. Tyber, V. Brice, C.P. Frick, H.J. Maier, N. Morgan, Tensile deformation of NiTi wires, *Mater. Res. Part A* 75 (2005) 810-823.
- [9] N. Zhou, C. Shen, M.F.-X. Wagner, G. Eggeler, M.J. Mills, Y. Wang, Effect of Ni_4Ti_3 precipitation on martensitic transformation in Ti-Ni, *Acta Materialia* 58 (2010) 6685-6694.

- [10] Y. Zhao, J. Zhang, Microstrain and grain-size analysis from diffraction peak width and graphical derivation of high-pressure thermomechanics, *J. Appl. Crystallogr.* 41 (2008) 1095-1108.
- [11] W. Woo, T. Ungar, Z. Feng, E. Kenik, B. Clausen, X-ray and neutron diffraction measurements of dislocation density and subgrain size in a friction-stir-welded aluminum alloy, *Metall. Mater. Trans. A* 41A (2010) 1210-1216.